Senescence Alters PPARG (Peroxisome Proliferator–Activated Receptor Gamma)-Dependent Fatty Acid Handling in Human Adipose Tissue Microvascular Endothelial Cells and Favors Inflammation

Anaïs Briot, Pauline Decaunes, Fanny Volat, Chloé Belles, Muriel Coupaye, Séverine Ledoux, Anne Bouloumié

Objective—Adipose tissue (AT) dysfunction associated with obesity or aging is a major cause for lipid redistribution and the progression of cardiometabolic disorders. Our goal is to decipher the contribution of human AT microvascular endothelial cells (ECs) in the maintenance of fatty acid (FA) fluxes and the impact of senescence on their function.

Approach and Results—We used freshly isolated primary microvascular ECs from human AT. Our data identified the endothelial FA handling machinery including FATPs (FA transport proteins) FATP1, FATP3, FATP4, and CD36 as well as FABP4 (FA binding protein 4). We showed that PPARG (peroxisome proliferator–activated receptor gamma) regulates the expression of FATP1, CD36, and FABP4 and is a major regulator of FA uptake in human AT EC (hATEC). We provided evidence that endothelial PPARG activity is modulated by senescence. Indeed, the positive regulation of FA transport by PPARG agonist was abolished, whereas the emergence of an inflammatory response was favored in senescent hATEC. This was associated with the retention of nuclear FOXO1 (forkhead box protein O1), whereas nuclear PPARG translocation was impaired.

Conclusions—These data support the notion that PPARG is a key regulator of primary hATEC function including FA handling and inflammatory response. However, the outcome of PPARG activation is modulated by senescence, a phenomenon that may impact the ability of hATEC to properly respond to and handle lipid fluxes. Finally, our work highlights the role of hATEC in the regulation of FA fluxes and reveals that dysfunction of these cells with accelerated aging is likely to participate to AT dysfunction and the redistribution of lipids. (***Arterioscler Thromb Vasc Biol*****. 2018;38:00-00. DOI: 10.1161/ATVBAHA.118.310797.)**

Key Words: adipose tissue ■ cellular senescence ■ endothelial cells ■ fatty acids ■ inflammation

Metabolic and cardiovascular disorders, seen as a leading cause for morbidity and mortality, are commonly associated with accumulation of fat mass in the central part of the body. White adipose tissue (WAT) dysfunction leading to incapacity to store the excess of fatty acids (FA) into neutral triglycerides, is recognized as a major contributor of type 2 diabetes mellitus because it promotes ectopic FA deposition and toxicity (lipotoxicity) in other metabolically active tissues such as the liver and skeletal muscle, leading to insulin resistance.[1] In turn, type 2 diabetes mellitus represents a strong risk factor for cardiovascular diseases and microvascular complications associated with profound dysfunction of endothelial cells (ECs).[2]

Premature aging of the WAT may be a causal event of its dysfunction.[3] Indeed, obesity and aging share common life-threatening disorders such as type 2 diabetes mellitus, hypertension, and cardiovascular diseases. In both conditions, WAT dysfunction is associated with an accumulation of senescent cells including progenitor (hPROG) cells that become unable to produce new fat cells[4,5] and consequently alters the ability of WAT to properly adapt to the influx of FA. Cellular senescence is at first a physiological mechanism in response to various stimuli such as DNA damage, oncogene activity, or metabolic stress, preventing the expansion of damaged cells. In particular, these cells, that become unable to proliferate, are characterized by the overexpression or activity of cell cycle inhibitors including the organismal aging marker P16INK4 (*CDKN2A*).[6] Although senescence could be protective against the development of diseases such as cancer, it is likely that accumulation of senescent cells may have deleterious impact.

FA, naturally stored as triglycerides in adipocytes, have to be channeled through the microvascular endothelium according to mechanisms that remain poorly understood. Transport of FA through nonfenestrated microvascular endothelium

Received on: July 17, 2017; final version accepted on: March 1, 2018.

From the Inserm, UMR1048, Team 1, I2MC, Institute of Metabolic and Cardiovascular Diseases, Université de Toulouse, France (A. Briot, P.D., F.V., C.B., A. Bouloumié); and Center Support of Obesity, Hôpital Louis Mourier, Colombes, France (M.C., S.L.).

The online-only Data Supplement is available with this article at http://atvb.ahajournals.org/lookup/suppl/doi:10.1161/ATVBAHA.118.310797/-/DC1.

Correspondence to Anaïs Briot, UMR1048 Inserm, Team 1, I2MC, Institute of Metabolic and Cardiovascular Diseases, Université de Toulouse, Toulouse 31432, France. E-mail anais.briot@inserm.fr

Nonstandard Abbreviations and Acronyms

AT	adipose tissue
EC	endothelial cell
FA	fatty acids
FABP	FA binding protein
FATP	FA transport protein
FOXO1	forkhead box protein O1
hATEC	human adipose tissue EC
hMA	human mature adipocytes
hPROG	progenitor
IL	interleukin
PPARG	peroxisome proliferator–activated receptor gamma
WAT	white AT

is believed to involve membrane FATPs (FA transporters; FATPpm, CD36) and cytoplasmic FABPs (FA binding proteins).[7,8] In the heart and skeletal muscle with high energy needs, FA transport through endothelial expression of FATP3 and FATP4 are locally regulated by VEGF-B. Importantly, blockade of VEGF-B signaling reverses insulin resistance in animal models of obesity.[9,10] Noticeably, this regulation was not observed in WAT ECs supporting that the mechanisms involved in FA handling vary across vascular beds. In WAT endothelium, other factors including PPARG (peroxisome proliferator–activated receptor gamma) have been proposed to play a role.[8,11]

PPARG is a ligand-activated transcription factor and the master regulator of adipogenesis.[12] Polymorphisms and mutations in *PPARG* gene are associated with the development of metabolic syndrome, illustrating its critical role in lipid homeostasis and metabolism.[13–15] PPARG-dependent pathway activation by thiazolidinediones is efficient to decrease blood glucose in diabetic subjects, restore insulin sensitivity, limit dyslipidemia, prevent ectopic deposition of FA, and hamper inflammation. However, these drugs have dramatic side effects leading to restriction in the United States and withdrawal in Europe.[16–18] We have observed in obese individuals that human AT EC (hATEC) from visceral AT exhibited higher senescent phenotype than subcutaneous AT and a decrease in *PPARG* expression.[19] Together these evidence led us to hypothesis that disruption of PPARG activity in senescent ECs contributes to the dysfunction of AT.

Using primary ECs freshly isolated from human AT, we characterized the FA handling machinery and ascertained the contribution of PPARG in the regulation of endothelial FA uptake in human subcutaneous AT. In addition, we observed that, with the progression of senescence, activation of PPARG drove differential response with a shift in the balance between FA fluxes and inflammation. These events were associated with a loss of PPARG nuclear translocation and retention of FOXO1 (forkhead box protein O1).

Altogether, our observations underline the critical role of ATEC in human, in the regulation of FA fluxes that have to be taken into account in the comprehension of disorders associated with FA redistribution and lipotoxicity and the development of future therapies.

Materials and Methods

Human AT and Isolation of the Cell Subtypes

Subcutaneous abdominal ATs were obtained from healthy adult women undergoing dermolipectomy for esthetic purposes. Paired matched visceral and subcutaneous AT biopsies were obtained through a cohort study including nonobese and obese subjects. These studies were approved by the Institutional Review Boards. All subjects provided written informed consent. Protocol is registered at ClinicalTrials.gov (SENADIP; URL: http://www.clinicaltrials.gov. Unique identifier: NCT01525472). Clinical parameters of the donors from this protocol are summarized in Table I in the online-only Data Supplement.

AT was prepared as previously described to obtain stroma-vascular cells and mature adipocytes (hMA).[20] Native hPROG and ECs from the stroma-vascular fraction were isolated by immunoselection/depletion; after the negative selection of immune cells (anti-CD45-depletion kit; StemCell technology), hPROG ($CD31^{NEG}$), and endothelial ($CD31^{POS}$) cells were then separated based on the immunoselection of $CD31^{POS}$ population (Dynabeads CD31 Endothelial Cell; ThermoFisher Scientific).

EC Culture and Treatments

hATEC were grown in Endothelial Cell Growth Medium MV (Promo Cell) supplemented with 50 µg/mL gentamicine (GIBCO) on tissue culture dishes coated with 2 $\mu g/cm^2$ fibronectin (Millipore). Rosiglitazone (3 µmol/L) and GW9662 (10 µmol/L; for 12 hours) were added or not to the media.

For FA uptake experiments, hATEC or stroma-vascular fraction was starved for 4 hours in HBSS 0.1% BSA FA free and then incubated with BODIPY FL C16 (750 nmol/L final) for 2, 10, and 30 minutes. Incorporation of fluorescent C16 was then measured by flow cytometry.

Transmission Electron Microscopy

Samples were fixed with 2% glutaraldehyde in Sorensen buffer (0.1 mol/L, pH=7.4) for 1 hour, washed with the Sorensen phosphate buffer (0.2 mol/L) for 12 hours and postfixed with 1% OsO_4 in Sorensen buffer (Sorensen phosphate, 0.05 mol/L; glucose, 0.25 mol/L; OsO_4, 1%) for 1 hour. Samples were dehydrated in an increasing ethanol series (up to 100% ethanol) and then with propylene oxide. Samples were embedded in epoxy resin (Epon 812). After 48 hours of polymerization at 60°C, ultrathin sections (70 nm) were mounted on 100 mesh collodion-coated copper grids and poststained with 3% uranyl acetate in 50% ethanol and with 8.5% lead citrate before being examined on an HT7700 Hitachi electron microscope at an accelerating voltage 80 KV.

Flow Cytometry

hPROG and hATEC were analyzed by flow cytometry using surface markers detected with antibodies CD45-BV510 (clone HI30, BioLegend), CD34-PerCP (clone 8612, BD), CD31-V450 (clone WM59, BD Horizon), FATP1-PE (clone 308420, R&D Systems), FATP4-APC (clone 342142, R&D Systems), and CD36-APC-Cy7 (Clone 5–271, BioLegend) or appropriate isotype controls. Cell suspensions were incubated with primary antibodies in PBS 2 mmol/L EDTA 0.5% BSA buffer. After a 20-minute incubation on ice, the cells were washed, resuspended, and analyzed on a FACS Canto II flow cytometer using Diva Pro software (BD Biosciences).

Transcriptional Analysis

Total RNA from hATEC and hPROG cells was purified using RNeasy Mini kit Plus (QIAGEN). Homogenization in Qiazol buffer (QIAGEN) was performed before isolating RNA from hMA. Complementary DNA synthesis was performed with Superscript II reverse transcriptase (Invitrogen) using random hexamers primers. Quantitative RT-PCR was performed using probe and primer sets

(Applied Biosystems) described in Table II in the online-only Data Supplement. Each reaction was run in duplicate with Takyon Low Rox Probe MasterMix dTTP Blue (Eurogentec) on a ViiA 7 (Applied Biosystems) thermocycler. *18S* and *PPIB* were used as housekeeping genes for native and cultured cells respectively.

Immunostaining

hATEC grown at confluence were fixed with 4% paraformaldehyde in PBS for 10 minutes at room temperature. For immunodetection VE-CADHERIN (clone C-19, Santa-Cruz Biotechnology), FOXO1 (Clone D7C1H, Cell Signaling), PPARG (Clone C26H12, Cell Signaling), and NFKB P65 (Clone L8F6, Cell Signaling No. 6956) primary antibodies were used to detect the proteins of interest in combination with appropriate secondary antibody Alexa Fluor-conjugated (Invitrogen). Nuclei were stained with DAPI. Cells were imaged using inversed fluorescent microscope Nikon Eclipse TE300 (Nikon) and NIS-Elements 2.5 BR software (Nikon; Figure 2) or with an inverted fluorescent confocal microscope ZEISS LSM780 (Software ZEN; Figures 6 and 7).

Western Blot Analysis

hATEC were lysed at passage 2 or 6 in modified RIPA buffer containing 1% Triton x-10 and 0.1% SDS. Five to 10 µg of protein lysate were resolved and analyzed by Western blot using the following primary antibodies: PPARG (Clone C26H12, Cell Signaling), FOXO1 (Clone D7C1H Cell Signaling), and β-TUBULIN (Clone D3U1W, Cell signaling) following the recommendations of the manufacturer. Quantification of bands by densitometry was performed using ImageLab Software (Bio-Rad Laboratories).

ECs From Human AT Transduced With SV40-AgT

Primary ECs ($CD45^{NEG}$, $CD34^{POS}$, and $CD31^{POS}$) from human AT were isolated from the stroma-vascular fraction by flow cytometry (BD Influx cell sorter; BD Bioscience) using the following combination of antibodies: CD45-BV510 (clone HI30, Biolegend), CD34-PerCP (clone 8612, BD), and CD31-V450 (clone WM59, BD Horizon). Sorted cells were allowed to recover overnight in Endothelial Cell Growth Medium MV medium, before infection with lentiviral particles expressing SV40-large T antigen (Applied Biological Materials Inc) in the presence of protamine sulfate (4 µg/mL).

Statistical Analysis

Statistical analyses were performed using Prism (GraphPad Software). Comparisons between 2 independent groups were performed using 2-tailed nonparametric *t* test (Mann–Whitney test). For matched groups, after variance analysis (*F* test), paired parametric or nonparametric (Wilcoxon test) 2-tailed *t* test was performed. Comparisons between passaged cells were performed using nonparametric ANOVA tests and Sidak multiple comparison posttests. Correlations were obtained using Spearman coefficient (Spearman test; Figure 5). Differences were considered statistically significant when $P<0.05$.

Results

FA Handling Machinery in Native hATECs

To better characterize the human WAT microvascular cells, we performed transmission electron microscopy. As shown in Figure 1A, we observed that the microvascular endothelium from human AT is nonfenestrated. Therefore, active mechanisms are most likely to be involved in the WAT transendothelial FA fluxes. To further study the FA handling machinery potentially involved in this active microvascular transport, we isolated native microvascular ECs from human abdominal subcutaneous AT (hATEC) based on cell surface markers ($CD45^{NEG}$/$CD34^{POS}$/$CD31^{POS}$). We confirmed by quantitative RT-PCR the high expression level of *CD31* and *GPIHBP1* (Figure 1B), an EC-specific protein involved in the luminal presentation of the lipoprotein lipase,[21] compared with hMA and hPROG cells ($CD45^{NEG}$/$CD34^{POS}$/$CD31^{NEG}$). Transcript levels of genes encoding FA transporters (FATP) 1 (*SLC27A1*) and FATP3 (*SLC27A3*) were lower in hMA compared with hATEC and hPROG, whereas *SLC27A4* (encoding FATP4) was similar in the 3 cell types (Figure 1C). Transcript levels of *FABP4* (also known as *aP2*) and *CD36* (also known as *FAT*) both PPARG-targeted genes, as well as *PPARG* itself,[22,23] were as expected more expressed in hMA than in hPROG cells. In addition, they were also strongly expressed in hATEC (Figure 1D).

Finally, we performed flow cytometry to analyze cell surface expression of FATP1, FATP4, and CD36 in native hPROG and hATEC (Figure 1E through 1I). FATP1 and FATP4 proteins were more exposed at the cell surface of hATEC than hPROG (Figure 1E, 1F, and 1H) although mRNA levels were similar (Figure 1C). In parallel, the amount of CD36 protein was 40-fold higher at the cell surface of hATEC than hPROG (Figure 1G and 1I). Therefore, native hATEC express actors of the FA handling machinery at levels comparable to adipocytes together with a significant exposure at the plasma membrane, supporting the role of hATEC in the regulation FA fluxes.

PPARG Is Critical for the Regulation of FA Uptake in hATEC

We have previously shown using a cohort of obese individuals, that *PPARG* expression level was decreased in EC from visceral AT compared with subcutaneous AT.[19] By flow cytometry performed on native hATEC, we observed that CD36 was also decreased at the surface of cells isolated from obese visceral AT (Ob Vs) compared with visceral AT from nonobese individuals (Ln Vs) and subcutaneous AT from obese individuals (Ob Sc; Figure 2A). This FA coreceptor was described to be regulated by PPARG activation in mouse endothelium[11] and human cardiac microvascular ECs in vitro.[24]

To further analyze FA handling in native hATEC, we measured by flow cytometry their ability to uptake fluorescent FA (Bodipy FL C16) in vitro (Figure 2B and 2C). At 37°C hATEC efficiently incorporated FA. This phenomenon was not observed when the cells were maintained at 4°C (Figure 2B). In the presence of PPARG agonist rosiglitazone at 37°C, a time-dependent increase in FA uptake was observed (rosi; Figure 2B and 2C) demonstrating that rosiglitazone treatment promotes FA uptake in hATEC.

To assess the contribution of PPARG in the rosiglitazone-mediated regulation of FA fluxes, we used a model of hATEC transduced with SV40-large T antigen ($hATEC^{SV40}$). In $hATEC^{SV40}$ the expression of EC markers including CD31 (Figure 2D) and VE-CADHERIN (Figure 2E; red) was maintained, but *PPARG* mRNA level was 5× lower than in primary hATEC (Figure 2F). Low expression of *PPARG* in $hATEC^{SV40}$ was associated with a significantly lower expression of *SLC27A1, FABP4*, and *CD36* (Figure 2F and 2G), described to be PPARG-dependent genes in other

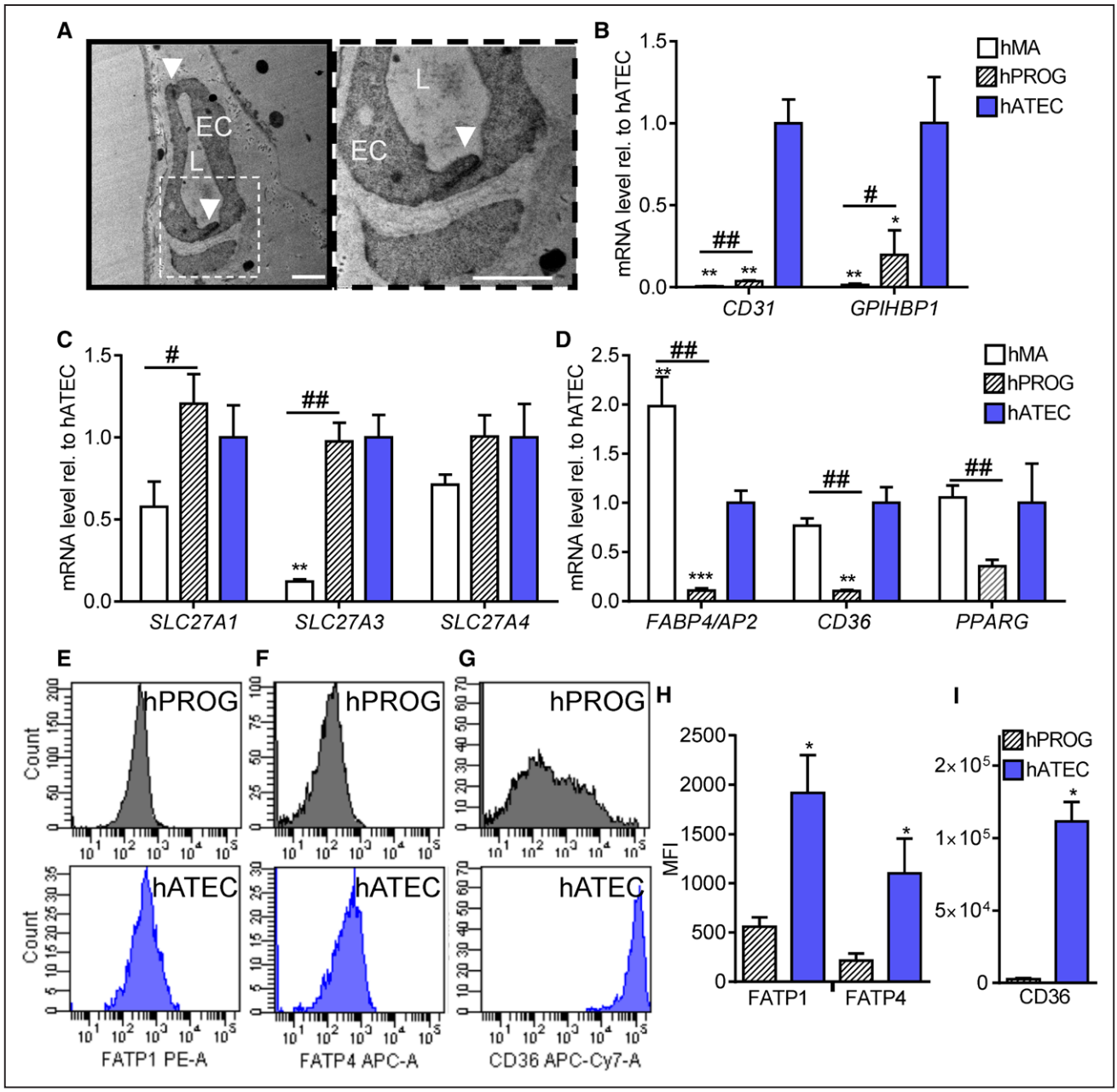

Figure 1. Fatty acid is handling machinery in native microvascular endothelial cells from human adipose tissue. **A**, Transmission electron microscopy picture of human adipose tissue capillary with cohesive tight cell–cell contacts (white arrows). EC indicates endothelial cell; and L, lumen; scale bars=10 μm. **B**–**D**, Transcriptional analysis of native human mature adipocytes (hMA), progenitor (hPROG), and microvascular endothelial (hATEC) cells was performed by qRT-PCR. mRNA levels are represented relative to average expression in hATEC. n=5 to 8 individuals. **P* value to hATEC; #*P* value between hPROG and hMA. **E**–**I**, Surface levels of FATP1 (fatty acid transport protein; **E**–**H**) and FATP4 (**F**–**H**) and CD36 (**G**–**I**) were evaluated by flow cytometry in paired native hPROG (**upper**) and hATEC (**lower**). Representative histograms of cell count to mean fluorescence intensity (MFI) are shown (**E**–**G**) and MFI detection is presented. n=6 to 7 donors. #,**P*<0.05; ##,***P*<0.01; ###,****P*<0.001. Data are presented as mean±SEM.

cell types.[22,23,25,26] To note, no changes were observed for *SLC27A4* (Figure 2F), which is not known as a PPARG responsive gene. In hATEC^{SV40}, rosiglitazone treatment was not effective in increasing the uptake of FA (Figure 2H). Finally, treatment of hATEC with an irreversible inhibitor of PPARG (GW9662) significantly decreased the impact of rosiglitazone on FA uptake (Figure 2H), strongly supporting the contribution of PPARG in endothelial FA uptake in human AT.

Replicative Senescence Alters the Induction of Endothelial FA Uptake by PPARG

To study the impact of EC senescence in PPARG-mediated FA handling, we performed serial passaging (P) of primary hATEC and studied their ability to uptake FA over time. Uptake of Bodipy FL C16 was measured by flow cytometry in primary hATEC from P2 to P6 grown in the presence or not of rosiglitazone (Figure 3A through 3C). Noticeably, in untreated cells (Figure 3A through 3C) hATEC exhibited a

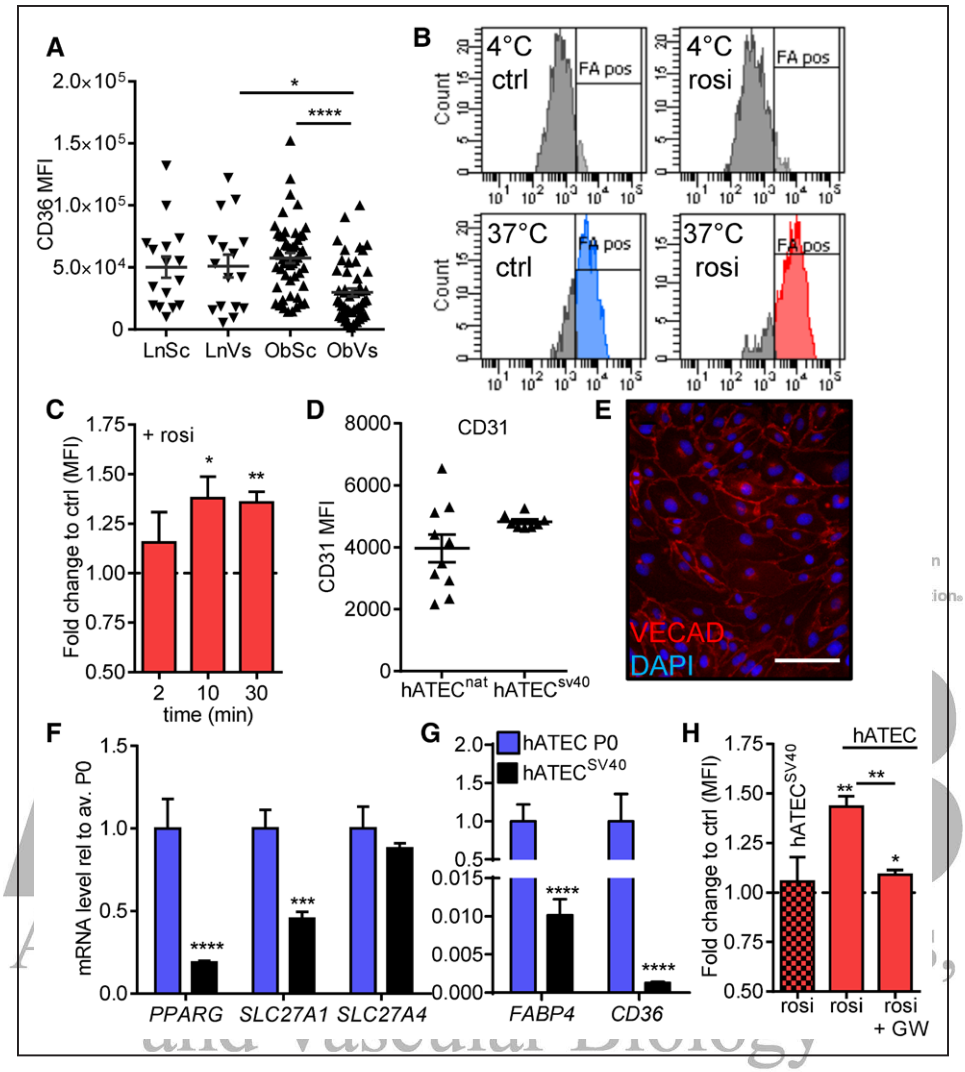

Figure 2. PPARG (peroxisome proliferator–activated receptor gamma) is critical for the regulation of fatty acid uptake in human adipose tissue endothelial cell (hATEC). **A**, CD36 was detected by flow cytometry (mean fluorescence intensity [MFI]) at the cell surface of native hATEC isolated from paired subcutaneous (Sc) and visceral (Vs) adipose tissue from nonobese (Ln; n=16) and obese (Ob; n=51) individuals. **B–C**, Uptake of Bodipy FL C16 (750 nmol/L) was assessed by flow cytometry in primary hATEC inside the stroma-vascular fraction grown in the presence or not of rosiglitazone (rosi; 3 µmol/L). Measurement was performed in the $CD45^{NEG}/CD34^{POS}/CD31^{POS}$ population. Representative histograms of cell count to MFI are shown (**B**); MFI of Bodipy FL in rosiglitazone-treated cells compared with control is shown (**C**). n=4 individuals. **D**, Immunodetection by flow cytometry of CD31 at the cell surface of human native ($hATEC^{nat}$; n=10) and SV40-AgT transduced ($hATEC^{SV40}$; n=8; 4 clones) endothelial cells from the adipose tissue. **E**, Immunodetection of VE-CADHERIN (VECAD; red) at the cell–cell junction in $hATEC^{SV40}$. Scale bar=100 µm. **F** and **G**, Transcript levels of genes of interest were measured by qRT-PCR in primary hATEC (P0; blue) and $hATEC^{SV40}$ (black). hATEC P0 n=6 (3 donors); $hATEC^{SV40}$ n=14 (4 clones). **H**, Uptake of Bodipy FL C16 (750 nmol/L) was assessed by flow cytometry in $hATEC^{SV40}$ and primary hATEC in the presence or not of rosiglitazone (3 µmol/L) and GW9662 (GW, 10 µmol/L; 12 hours). Mean fluorescence intensity of Bodipy FL (MFI) in rosiglitazone-treated cells compared with control is shown at 30 min. n=4. *P<0.05; **P<0.01; ***P<0.001; ****P<0.0001. Data are presented as mean±SEM.

progressive decrease in FA uptake efficiency. Furthermore, although PPARG activation (Figure 3A through 3C) enhanced FA uptake at early passage (P2; Figure 2A), the positive regulation was lost with cell passaging (P3/4 and P5/6; Figure 3B and 3C). Passaging and treatment with rosiglitazone had no noticeable effect on the amount of FATP1 and FATP4 presented at the cell surface (Figure 3D through 3G). In contrast, rosiglitazone treatment increased the amount of CD36 detected at the cell surface at early passage, but the positive regulation was progressively lost with passaging (Figure 3H and 3I). Treatment with rosiglitazone did not modify the cell surface expression of neither FATPs nor CD36 in $hATEC^{SV40}$ (Figure 3D through 3I). This suggests thats replicative senescence in hATEC abolishes the induction of FA uptake together with the presentation of CD36 at the plasma membrane mediated by PPARG agonist.

Replicative Senescence Abrogates the Transcriptional Induction of FA Handling Machinery by PPARG

Blockade of rosiglitazone-induced FA uptake in primary hATEC after passage 3/4 was not associated with a decrease in *PPARG* expression (Figure 4A). However, serial passaging induced a rapid and significant upregulation of the senescence

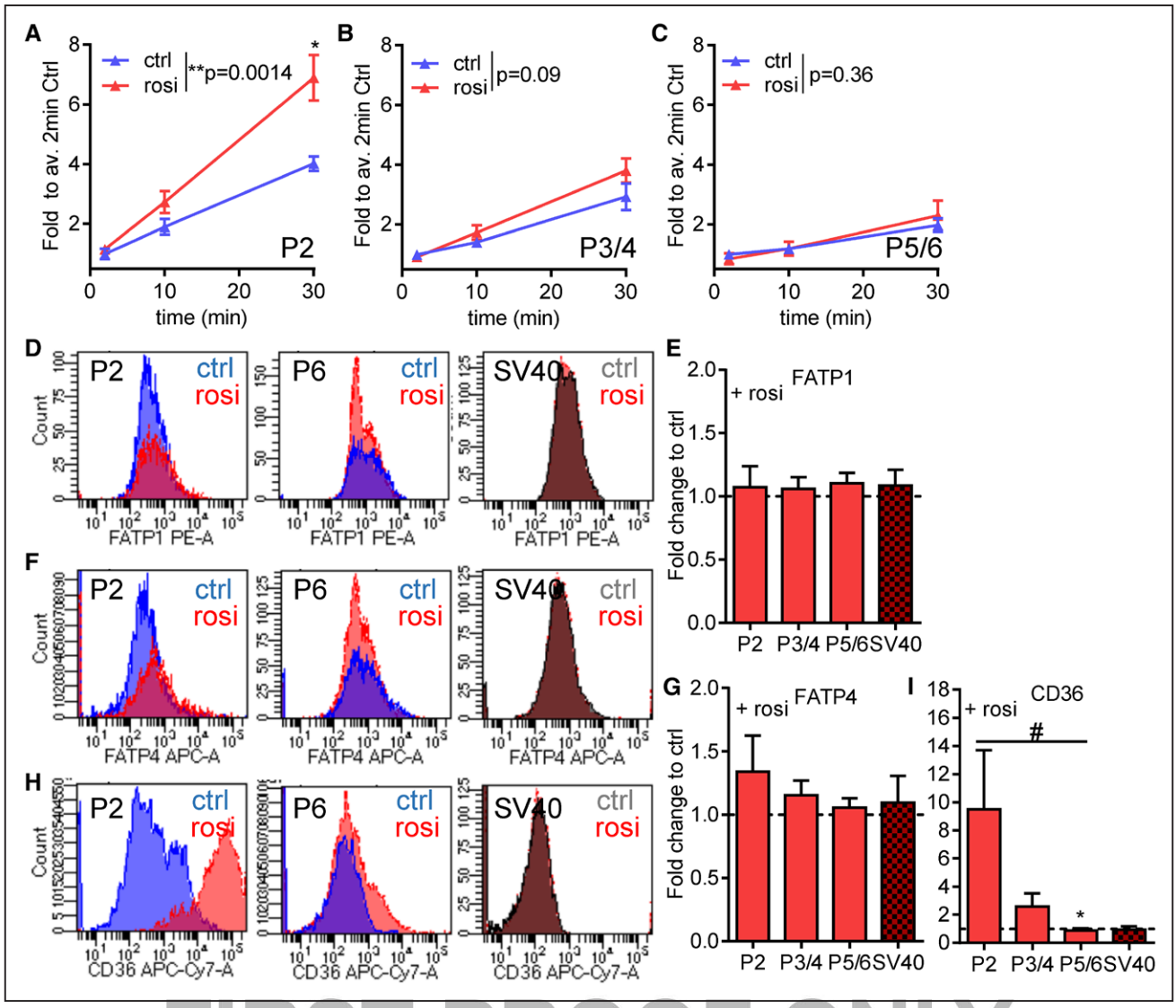

Figure 3. Replicative senescence alters endothelial fatty acid (FA) uptake in response to PPARG (peroxisome proliferator–activated receptor gamma) activation. **A**–**C**, Uptake of Bodipy FL C16 (750 nmol/L) was assessed by flow cytometry in primary human adipose tissue endothelial cell (hATEC; n=3–4 donors) from passage (P) 2 to 6 in the presence (red) or not (blue) of rosiglitazone (rosi; 3 μmol/L). Overtime increase of fluorescence compared with average 2-minute controls is represented ±SEM. **D**–**I**, Surface expression of FATP1 (fatty acid transport protein; **D**–**E**), FATP4 (**F**–**G**), and CD36 (**H**–**I**) was measured by flow cytometry in hATEC from passage (P) 2 and 6 (n=3–4 donors) and in hATEC^{SV40} (SV40; n=4) in the presence (red) or not of rosiglitazone (3 μmol/L). Representative histograms of cell count to mean fluorescence intensity are shown (**D**, **F**, and **H**). Mean fluorescence intensity of Bodipy FL (MFI) in rosiglitazone-treated cells compared with control is shown as ±SEM. #*P*<0.05; **P*<0.05 compares P2 to P5/6.

marker *CDKN2A* (encoding P16INK4) that reached up to 120-fold at P5/6 compared with P0. These levels were nevertheless significantly lower than in hATEC^{SV40} in which *CDKN2A* was >2000-fold higher than in primary P0 cells (Figure 4B). To explore the cause behind the loss of FA uptake in these cells, we performed transcriptional analyses on serially passaged (P0 to P6) primary hATEC grown in the presence or not of rosiglitazone. Treatment with rosiglitazone robustly induced the expression of *SCL27A1, FABP4*, and *CD36* (Figure 4C and 4D) in primary hATEC at P0. In hATEC^{SV40}, *CD36* and *FABP4* were responding to PPARG activation although 5- to 10-fold less than in primary cells. In addition, rosiglitazone treatment failed to induce *SLC27A1* and to maintain a *PPARG* positive feedback loop in hATEC^{SV40} (Figure 4C through 4E). Finally, the involvement of PPARG in rosiglitazone-mediated transcriptional regulation of *SLC27A1*, *CD36*, and *FABP4*, as well as *PPARG*, was further confirmed by the use of the irreversible PPARG antagonist GW9662 in primary hATEC (Figure 4F).

In contrast to the effect measured at P0, the induction *SLC27A1*, *FABP4*, and *CD36* by rosiglitazone was progressively lost with passaging (Figure 4C and 4D). In addition, the feedback loop of *PPARG* expression was also affected with an inversion of the balance between P1/2 and P3/4 (Figure 4E). *SLC27A4*, which expression is independent of PPARG activity, was not significantly changed (Figure 4C). Noticeably, the pattern of this transcriptional deregulation coincided with the functional defect in FA uptake induction that progressively

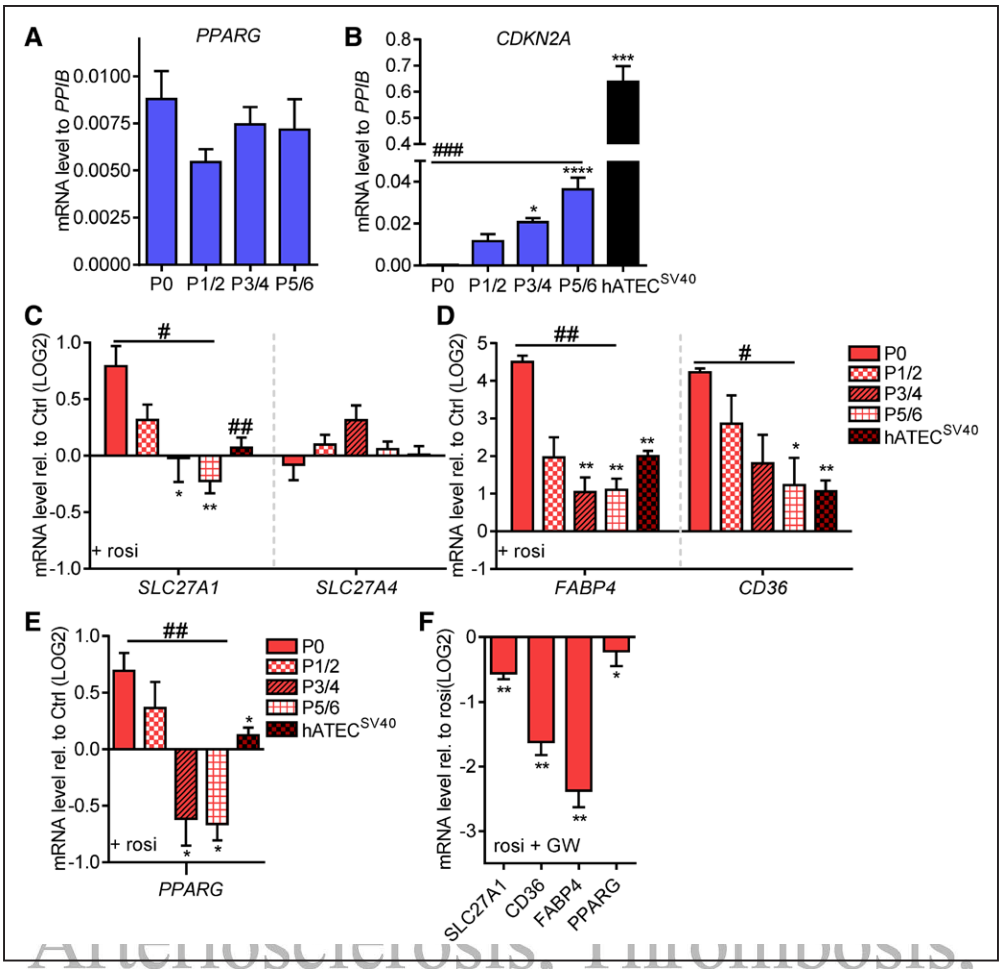

Figure 4. Replicative senescence abrogates the transcriptional induction of fatty acid (FA) handling machinery by PPARG (peroxisome proliferator–activated receptor gamma). Primary human adipose tissue endothelial cell (hATEC) were serially passaged (P) up to 6×. **A** and **B**, Transcript levels of *PPARG* and *CDKN2A* were measured by qRT-PCR and represented as relative to housekeeping gene (*PPIB*) expression in primary hATEC (blue; P0 to P6) or hATEC^{SV40} (black; B). hATEC n=4 donors; hATEC^{SV40} n=14 (4 clones). ###*P*<0.001; **P*<0.05, ****P*<0.001, *****P*<0.0001 compared with P0 hATEC. **C**–**E**, Primary hATEC from passage (P) 0 to 6 or hATEC^{SV40} were treated or not with rosiglitazone (3 μmol/L). Transcript levels of genes involved in FA handling were measured by qRT-PCR. Fold induction compared with untreated controls are represented in LOG2 scale. hATEC n=4 donors; hATEC^{SV40} n=7 (4 clones). #*P*<0.05; ##*P*<0.01. **P*<0.05, ***P*<0.01 compares to P0. **F**, P0/P1 primary hATEC were treated with rosiglitazone in the presence or not of GW9662 (10 μmol/L). Fold induction compared with rosiglitazone-treated cells are represented in LOG2 scale. n=3 donors. Data are presented as mean±SEM.

occurred between P2 and P5/6 (Figure 3). These data support that the alteration of PPARG transcriptional activity participates to the deregulation of FA handling in hATEC.

CDKN2A Accumulates in Native hATEC With Aging and Its Expression Correlates With a Decrease in Responsiveness to PPARG Activation

The cyclin inhibitor P16INK4 (encoded by *CDKN2A*) has been shown in various systems to accumulate with senescence and aging.[6,27] In a cohort of 28 individuals, we studied the expression pattern of *CDKN2A* in freshly isolated native hATEC from abdominal subcutaneous AT. Noticeably, we found that increasing levels of *CDKN2A* was positively correlated with aging (Figure 5A).

To further examine the link between hATEC senescence and their ability to respond and regulate FA fluxes, we performed correlation studies between the expression of *CDKN2A* and genes encoding the FA handling machinery, independently of replication cycle. hATEC transcriptional profile was evaluated under rosiglitazone treatment to mimic the activation of PPARG that may occur in response to circulating lipid by-products and FA released from adipocytes. In primary hATEC, we observed a strong inversed correlation between *CDKN2A* level and the expression of PPARG-target genes *SLC27A1*, *CD36*, and *FABP4* (Figure 5B, 5D, and 5E). The expression of PPARG-independent FA transporter *SLC27A4* was not correlated with *CDKN2A* pattern (Figure 5C). Thus, under increasing senescence pressure and aging, hATEC may progressively lose PPARG-mediated ability to adapt and regulate FA fluxes.

Replicative Senescence Induces a Shift in the Response to PPARG Activation in Primary hATEC

In parallel to the hampered induction of FA handling machinery that occurred in senescent hATEC, we observed an unexpected change in PPARG transcriptional regulatory activity.

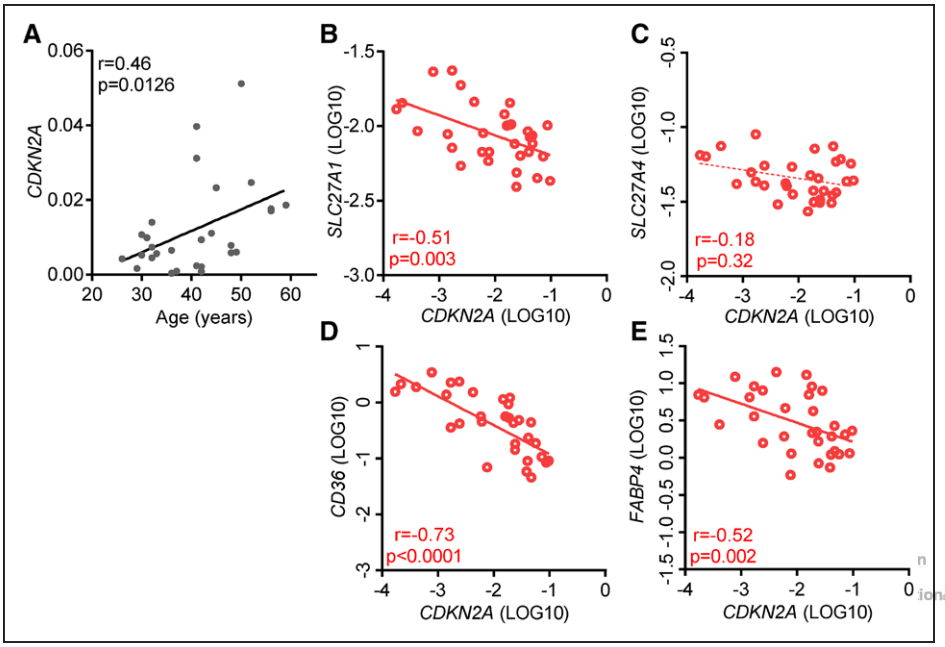

Figure 5. *CDKN2A* accumulates in human adipose tissue endothelial cell (hATEC) with aging and correlates with a decrease in fatty acid (FA) handling machinery expression in response to PPARG (peroxisome proliferator–activated receptor gamma) activation. **A**, *CDKN2A* transcript levels were measured in native hATEC isolated from abdominal subcutaneous adipose tissue of 26 to 69-year-old individuals. Correlation strength between *CDKN2A* and age was assessed by Spearman *r* calculation. n=28 individuals. **B–E**, Transcript levels of *CDKN2A*, *SLC27A1*, *SLC27A4*, *CD36*, and *FABP4* were measured in primary hATEC from passage P0 to P6 in the presence of rosiglitazone (3 μmol/L). Expression levels relative to housekeeping gene are presented in LOG10 scale. Spearman *r* and *P* values are shown. n=32 (8 donors).

Indeed, PPARG activation by rosiglitazone at P0 efficiently repressed the expression of genes encoding mediators of senescence such as *CCND1* (encoding cyclin D1) and *IGFBP3*. This effect was lost with passaging and even led to the induction of the latest. The expression of *SIRT1* and *CDKN2A* were not regulated by PPARG activation (Figure 6A). In addition, the anti-inflammatory effect of PPARG activation was also rapidly lost with passaging and instead triggered the induction of inflammatory mediators such as *ICAM1* and *MCP1* together with a tendency to promote the upregulation of *IL* (interleukin)-6 and IL-8 at late passages (Figure 6B). These changes were likely dependent of PPARG as this was not happening in hATEC^{SV40} (Figure 6A and 6B) that exhibit low levels of the transcription factor.

PPARG has been shown to antagonize NFKB activity through the transcriptional regulation of *NFKBIA* (encoding IKB alpha), competitive inhibition on the promoter of target genes or NFKB nuclear exclusion.[28,29] In hATEC, there were no significant changes in *NFKIA* expression with passaging (Figure 6C). In addition, in this cell type, *NFKIA* expression was barely regulated by rosiglitazone treatment (Figure 6D). However, by immunofluorescence staining, we noticed that the number of nuclei positive for NFKB-P65 subunit was increased by ≈3-fold in response to rosiglitazone in P6 hATEC, unlike what we observed in P2 hATEC (Figure 6E and 6F). This likely participated to the upregulation of known NFKB target genes, including *MCP1* and I*CAM1*. Altogether these observations support the notion that replicative senescence in hATEC may favor the emergence of proinflammatory and prosenescent events in response to PPARG agonist rosiglitazone.

Nuclear Translocation of PPARG Is Negatively Impacted by Replicative Senescence

Between P2 and P6, no change was observed in the expression of *PPARG* at the transcript (Figure 4A) and protein level (Figure 7A and 7B) that could account for the disrupted induction of its target genes. We thus assessed its subcellular localization by immunofluorescence staining. We observed that at early passage (P2), rosiglitazone treatment promoted a robust nuclear translocation of PPARG. However, in rosiglitazone-treated P6 hATEC, PPARG nuclear translocation was dramatically decreased (Figure 7C and 7G) an alteration that coincided with the decreased transcriptional activation of its target genes.

To further understand the decrease of nuclear PPARG in P6 hATEC, we focused our attention on FOXO1, a transcription factor previously shown to antagonize PPARG expression and activity.[30–32] At the transcript level, *FOXO1* was slightly increased with passaging. However, no significant regulation was observed between early (P1/2) and late passages (P5/6) (Figure 7D). In contrast, FOXO1 protein revealed a trend to accumulate at late passage (P6; Figure 7E and 7F). We then studied the subcellular localization of FOXO1 in combination with PPARG by immunofluorescence staining in P2 and P6 hATEC treated or not with rosiglitazone (Figure 7G through 7J). We noticed that at early passage (P2), rosiglitazone treatment decreased the proportion of nuclei single positive for FOXO1, as it may be expected about the reciprocal antagonistic effect of FOXO1 and PPARG. This effect was significantly hampered at P6 (Figure 7H through 7J), suggesting that in senescent hATEC, the retention of FOXO1 in the nuclei may

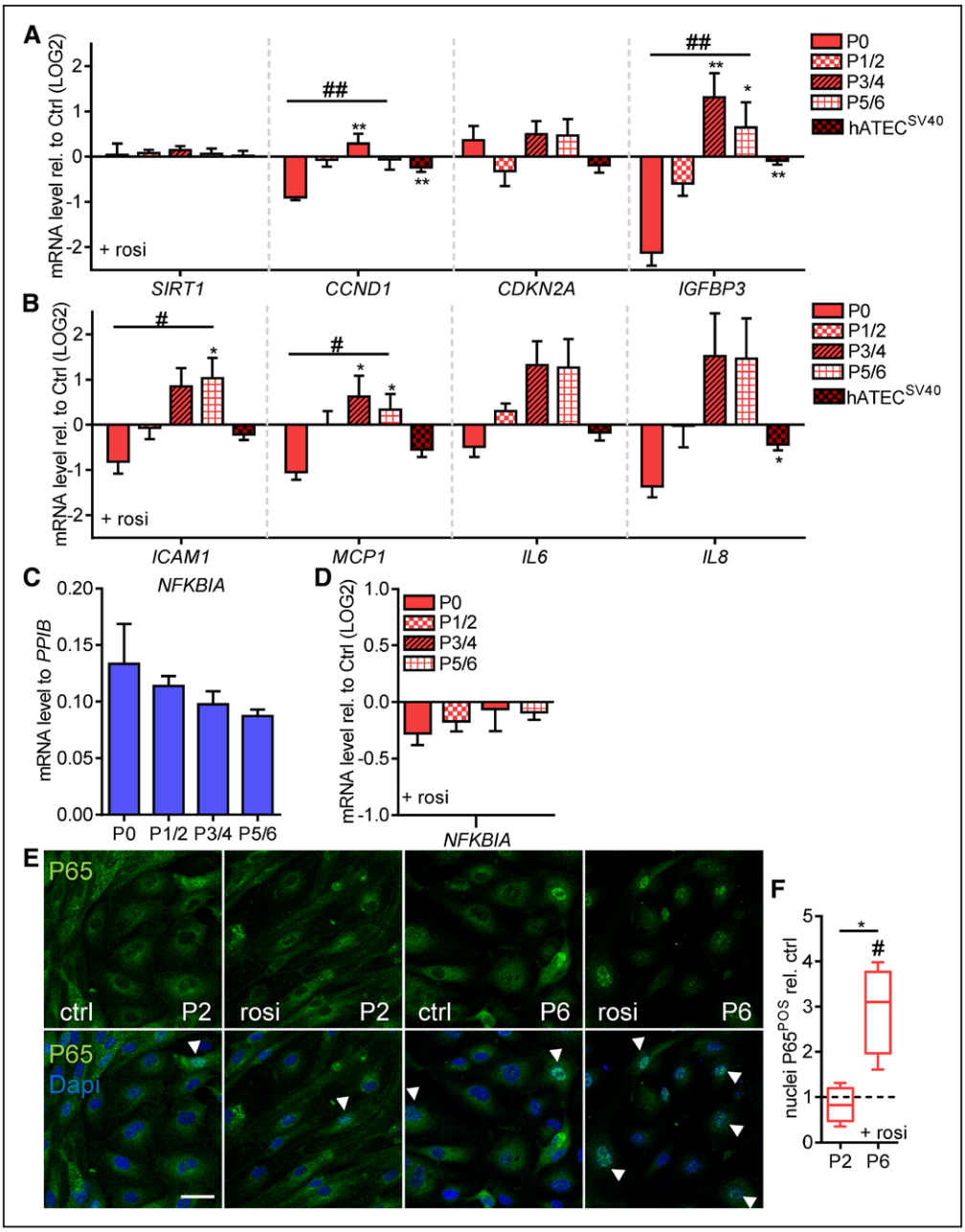

Figure 6. Replicative senescence promotes a transcriptional shift in response to PPARG (peroxisome proliferator–activated receptor gamma) activation. Primary human adipose tissue endothelial cell (hATEC) from passage (P) 0 to 6 or hATEC^{SV40} were treated or not with rosiglitazone (3 μmol/L). Transcript levels of genes involved in senescence (**A**) and inflammatory response (**B** and **D**) were measured by qRT-PCR. Fold induction compared with untreated controls are represented in LOG2 scale ±SEM. hATEC n=4 donors; hATEC^{SV40} n=7 (4 clones). #P<0.05; ##P<0.01. *P<0.05, **P<0.01 compares to P0. **C**, mRNA level of *NFKBIA* was measured by qRT-PCR and represented as relative to housekeeping gene (*PPIB*) in primary hATEC from P0 to P6. n=4 donors. **E** and **F**, NFKB-P65 subunit was detected by immunofluorescence (**E**, green) in native hATEC at P2 and P6 in the presence or not of rosiglitazone (rosi, 3 μmol/L). The number (%) of positive nuclei in rosiglitazone-treated hATEC compared with untreated controls are presented. #P<0.05 relative to untreated; *P<0.05 between P2 and P6. n=4 donors. Scale bar=40 μm.

contribute to alter PPARG nuclear translocation and maintenance and its transcriptional activity.

Discussion

ECs lining the lumen of blood microvessels relay physiological and pathological clues to the surrounding tissue. It is now well accepted that their phenotype and function are as various as the organs in which they reside.[33] Among vascular beds, the role of EC from the AT (ATEC) remains poorly understood. Using human primary ATEC, we demonstrated that PPARG activation increases FA uptake and FA handling machinery expression. Moreover, we showed that replicative senescence impacts hATEC responsiveness to ligand-mediated PPARG activation resulting into a shift in EC phenotype from active FA transporter cells toward proinflammatory activated cells.

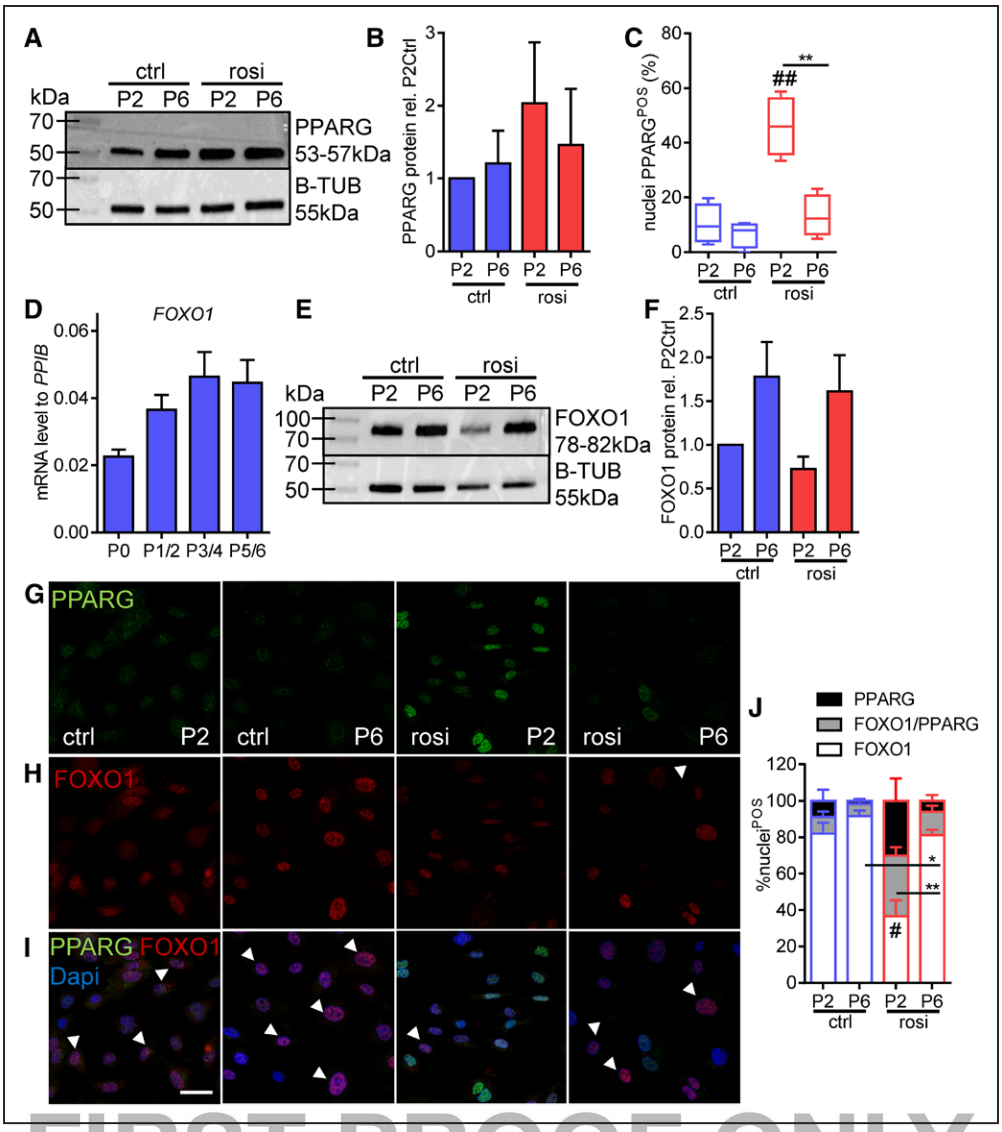

Figure 7. PPARG (peroxisome proliferator–activated receptor gamma) nuclear translocation is affected by senescence and coincides with FOXO1 (forkhead box protein O1) retention. Primary human adipose tissue endothelial cell (hATEC) from P0 to P6 were treated or not with rosiglitazone (rosi, 3 μmol/L). Protein levels of PPARG (**A** and **B**) and FOXO1 (**E** and **F**) were measured by Western blot. β-TUBULIN (B-TUB) was used as loading control. n=4 donors. **D**, mRNA level of *FOXO1* was measured by qRT-PCR and represented as relative to housekeeping gene (*PPIB*) in primary hATEC from P0 to P6. n=4 donors. Immunodetection of PPARG (green; **G** and **I**) and FOXO1 (red; **H** and **I**) were performed. Nuclei positive cells for PPARG are expressed as percent of cell number for each individual (**C**). **I**, White arrowheads: nuclei single positive for FOXO1. **J**, The repartition of PPARG, FOXO1, and PPARG/FOXO1 positive nuclei is presented ±SEM. For FOXO1 single positive nuclei: #$P<0.05$ compared with P2 ctrl; *$P<0.05$ between conditions for FOXO1 single positive nuclei. n=4 donors. Scale bars=40 μm.

The microcirculation is an active component of AT homeostasis. Dense with each adipocyte surrounded by a capillary, the blood vasculature is thought to follow AT growth. Although blocking the growth of blood vessels was first proposed to reduce fat mass expansion and improve obesity,[34] this strategy is now debated. Indeed, ATEC play multiple roles and targeting their expansion during the early phase of diet-induced obesity aggravates insulin resistance in mice.[35] In addition, recent studies highlighted the role of endothelial extracellular matrix in AT distribution, expansion, and systemic response to high fat diet in zebrafish.[36] Other works performed in mice also reported a role for ECs in WAT browning and thermogenesis.[37] Another facet of EC function is the regulation of metabolic fluxes including FA.[8] In the AT, the microvascular endothelium is the platform for lipoproteins hydrolysis. Although blockade of FA transport toward the adipocytes may be beneficial to prevent excessive fat storage and obesity, it may also favor an increase in circulating lipids, ectopic lipid deposition in other organs and the emergence of cardiometabolic disorders, including type 2 diabetes mellitus and atherosclerosis. In the present study, we showed that native human ATEC robustly express molecules involved in FA handling at similar to higher levels than the surrounding adipocytes and hPROG cells. In particular, high levels of PPARG-target genes *FABP4* and *CD36* commonly used as adipocyte markers and PPARG itself were detected

in hATEC. Our data also support that hATEC are key players in the appropriate handling of lipids and that this function is in part because of the activity of PPARG and presentation at the cell surface of FA transporters including CD36. These data collected in primary human ATEC are in agreement with previous observations made in mice carrying endothelial deletion of *Pparg*. Indeed, these animals exhibited a decrease in endothelial CD36 expression and a restriction in fat mass gain when fed a high fat diet.[11]

The central role of PPARG in lipid homeostasis is underlined by the association of *PPARG* mutations with lipodystrophy and metabolic syndrome conditions including dyslipidemia. In addition, PPARG-activating therapies have shown beneficial outcome in restoring glucose and lipid homeostasis in subjects with type 2 diabetes mellitus. Here, we provide evidence that the consequences of ligand-mediated PPARG activation in ECs is impacted by senescence. Senescence, evaluated by the expression of *CDKN2A* (encoding P16INK4), is increased with aging in native hATECs from subcutaneous AT. In vitro, the gradual increase in the expression of *CDKN2A*, because of serial passaging led to a progressive decrease in the metabolic response paralleled with an increase in the proinflammatory state in response to PPARG agonist. To note, over a certain threshold of senescence, as observed in hATEC^{SV40} and in native hATEC from obese visceral AT,[19] the expression of PPARG itself is dramatically reduced together with the one of CD36 at the cell surface. It is thus tempting to speculate that irreversible alterations of hATEC to handle FA may occur with disease and aging progression. PPARG is regulated by lipid by-products and thus likely participates to the endothelial response and adaptation to FA fluxes coming both from the blood and adipocytes. Consequently, one can expect that the deregulation of endothelial PPARG-dependent mechanisms would interfere both with the entry and the release of FA from the AT, ultimately favoring local and systemic dysfunctions. In our study, we addressed the impact of senescence on ligand-mediated PPARG response. To note, PPARG also exhibits ligand-independent activity including the recruitment of corepressor complexes to the promoter of target genes.[29,38] Previous studies also reported that PPARG without agonist binding displays transcriptional activity.[39] The PPARG N-terminal domain may contribute to this effect with a higher potency for the adipocyte-specific PPARG2 compared with PPARG1 isoform.[40] Furthermore, other works highlighted the role of kinases in ligand-independent activation of PPARG.[41,42] Thus, it is tempting to speculate that EC senescence, in addition to altering ligand-dependent PPARG response, may also impact ligand-independent PPARG activity. Further study will be needed to decipher the respective involvement of both mechanisms.

The change in endothelial ligand-induced PPARG response may also affect the surrounding cells through the secretion of IGFBP3, previously shown to promote insulin resistance,[43,44] as well as inflammatory cytokines MCP1, IL-6, and IL-8. It may be considered that the promotion of an inflammatory response in aging tissue may be a compensatory mechanism to adjust the surveillance of damaged and senescent cells. Indeed, the removal of senescent cells by genetic or pharmacological approaches has been shown to preserve AT function, insulin sensitivity, and improve metabolic parameters.[45–48]

The molecular events behind the differential response to PPARG agonist with senescence remain to be identified and may result from profound and complex changes in cellular landscape. Indeed, the effect of ligand-dependent activation of PPARG can be impacted by posttranslational modification of the receptor itself but also by the availability of a variety of cofactors that may account for the specificity of the response.[28,49] In hATEC, senescence was not associated with major changes in PPARG protein level. However, PPARG presence in the nucleus was dramatically decreased and coincided with the accumulation of FOXO1. Noticeably, defects in FOXO1 expression and activity in various organs have been previously linked to the development of a panel of diabetes mellitus–associated complications.[50] In the AT, FOXO1 interferes with PPARG activity[30–32,51,52] and antagonizes adipocyte differentiation. Mice expressing a dominant-negative form of FOXO1 under the control of the aP2 promoter showed improved glucose tolerance and insulin sensitivity.[51] Because aP2 is also expressed in ATEC, it is not excluded that some of these effects may be relayed through the endothelium. Similarly to PPARG, FOXO1 activity is mainly controlled by posttranslational changes that modulate its cellular localization, nucleic acid, and protein binding affinity. It is thus likely that alteration of hATEC functionality with senescence results primarily from protein modifications that ultimately promote a breakage of homeostatic regulatory loop between PPARG and FOXO1.[31,32]

As one of the first regulatory barrier between circulating metabolites and AT, ATEC have to be considered for the development of therapies aiming at restoring AT function and limiting lipotoxicity. Previous study in normoglycemic individuals has shown that rosiglitazone treatment had a positive impact on capillary density in periumbilical AT.[53] As underlined by the authors, this may participate to the improvement of insulin sensitivity through the delivery and removal of nutrient from the AT. Our study suggests that in addition, the positive effect of rosiglitazone on AT function may also be because of the regulation of transendothelial FA fluxes.

Combined with others, our data highlight the central role of AT endothelium in the maintenance of appropriate FA body distribution. However, the biological outcome of PPARG-dependent mechanisms in ECs may vary with disease progression and aging, a phenomenon that has to be considered for the development of therapies. Although insulin sensitization by PPARG agonists is efficient in metabolically active cells, we showed that ECs from the AT may also contribute to this response through the regulation of FA fluxes. Thus, in progress made to develop specific PPARG-activating drugs, the endothelium should not be disregarded.

Acknowledgments

We wish to acknowledge the contribution of TRI (Flow cytometry, Imaging) and GeT-TQ (transcriptomic) core facilities at I2MC; CMEAB (Center for Electron Microscopy applies to Biology, Faculté de Médecine Rangueil, Université de Toulouse III Paul Sabatier). We gratefully thank the Department of Plastic Surgery (Hôpital Universitaire Toulouse Rangueil, Toulouse, France), the

Center Support of Obesity and the Obstetrics and Gynecology Service (Hôpital Louis Mourier, F-92700, Colombes, France) for their involvement in adipose tissues collection. A. Briot designed research studies, conducted experiments, acquired and analyzed data, and wrote the article; P. Decaunes, F. Volat, and C. Belles were conducted experiments, acquired data, and analyzed data; M. Coupaye and S. Ledoux managed clinical studies; and A. Bouloumié designed research studies, analyzed data, and wrote the article.

Sources of Funding

This study was supported by funds from the French National Institute for Health and Medical Research (Inserm), the French Foundation for Medical Research (FRM), Clarins and Astra Zeneca.

Disclosures

None.

References

1. Schaffer JE. Lipotoxicity: when tissues overeat. *Curr Opin Lipidol*. 2003;14:281–287. doi: 10.1097/01.mol.0000073508.41685.7f.
2. Roberts AC, Porter KE. Cellular and molecular mechanisms of endothelial dysfunction in diabetes. *Diab Vasc Dis Res*. 2013;10:472–482. doi: 10.1177/1479164113500680.
3. Minamino T, Orimo M, Shimizu I, Kunieda T, Yokoyama M, Ito T, Nojima A, Nabetani A, Oike Y, Matsubara H, Ishikawa F, Komuro I. A crucial role for adipose tissue p53 in the regulation of insulin resistance. *Nat Med*. 2009;15:1082–1087. doi: 10.1038/nm.2014.
4. Stout MB, Justice JN, Nicklas BJ, Kirkland JL. Physiological aging: links among adipose tissue dysfunction, diabetes, and frailty. *Physiology (Bethesda)*. 2017;32:9–19. doi: 10.1152/physiol.00012.2016.
5. Tchkonia T, Morbeck DE, Von Zglinicki T, Van Deursen J, Lustgarten J, Scrable H, Khosla S, Jensen MD, Kirkland JL. Fat tissue, aging, and cellular senescence. *Aging Cell*. 2010;9:667–684. doi: 10.1111/j.1474-9726.2010.00608.x.
6. Campisi J. Senescent cells, tumor suppression, and organismal aging: good citizens, bad neighbors. *Cell*. 2005;120:513–522. doi: 10.1016/j.cell.2005.02.003.
7. Hagberg C, Mehlem A, Falkevall A, Muhl L, Eriksson U. Endothelial fatty acid transport: role of vascular endothelial growth factor B. *Physiology (Bethesda)*. 2013;28:125–134. doi: 10.1152/physiol.00042.2012.
8. Mehrotra D, Wu J, Papangeli I, Chun HJ. Endothelium as a gatekeeper of fatty acid transport. *Trends Endocrinol Metab*. 2014;25:99–106. doi: 10.1016/j.tem.2013.11.001.
9. Hagberg CE, Falkevall A, Wang X, et al. Vascular endothelial growth factor B controls endothelial fatty acid uptake. *Nature*. 2010;464:917–921. doi: 10.1038/nature08945.
10. Hagberg CE, Mehlem A, Falkevall A, et al. Targeting VEGF-B as a novel treatment for insulin resistance and type 2 diabetes. *Nature*. 2012;490:426–430. doi: 10.1038/nature11464.
11. Kanda T, Brown JD, Orasanu G, Vogel S, Gonzalez FJ, Sartoretto J, Michel T, Plutzky J. PPARgamma in the endothelium regulates metabolic responses to high-fat diet in mice. *J Clin Invest*. 2009;119:110–124. doi: 10.1172/JCI36233.
12. Tontonoz P, Graves RA, Budavari AI, Erdjument-Bromage H, Lui M, Hu E, Tempst P, Spiegelman BM. Adipocyte-specific transcription factor ARF6 is a heterodimeric complex of two nuclear hormone receptors, PPAR gamma and RXR alpha. *Nucleic Acids Res*. 1994;22:5628–5634.
13. Barroso I, Gurnell M, Crowley VE, Agostini M, Schwabe JW, Soos MA, Maslen GL, Williams TD, Lewis H, Schafer AJ, Chatterjee VK, O'Rahilly S. Dominant negative mutations in human PPARgamma associated with severe insulin resistance, diabetes mellitus and hypertension. *Nature*. 1999;402:880–883. doi: 10.1038/47254.
14. Claussnitzer M, Dankel SN, Klocke B, et al; DIAGRAM+Consortium. Leveraging cross-species transcription factor binding site patterns: from diabetes risk loci to disease mechanisms. *Cell*. 2014;156:343–358. doi: 10.1016/j.cell.2013.10.058.
15. Jeninga EH, Gurnell M, Kalkhoven E. Functional implications of genetic variation in human PPARgamma. *Trends Endocrinol Metab*. 2009;20:380–387. doi: 10.1016/j.tem.2009.04.005.
16. Ahmadian M, Suh JM, Hah N, Liddle C, Atkins AR, Downes M, Evans RM. PPARγ signaling and metabolism: the good, the bad and the future. *Nat Med*. 2013;19:557–566. doi: 10.1038/nm.3159.
17. Kung J, Henry RR. Thiazolidinedione safety. *Expert Opin Drug Saf*. 2012;11:565–579. doi: 10.1517/14740338.2012.691963.
18. Nissen SE, Wolski K. Effect of rosiglitazone on the risk of myocardial infarction and death from cardiovascular causes. *N Engl J Med*. 2007;356:2457–2471. doi: 10.1056/NEJMoa072761.
19. Villaret A, Galitzky J, Decaunes P, Estève D, Marques MA, Sengenès C, Chiotasso P, Tchkonia T, Lafontan M, Kirkland JL, Bouloumié A. Adipose tissue endothelial cells from obese human subjects: differences among depots in angiogenic, metabolic, and inflammatory gene expression and cellular senescence. *Diabetes*. 2010;59:2755–2763. doi: 10.2337/db10-0398.
20. Estève D, Boulet N, Volat F, et al. Human white and brite adipogenesis is supported by MSCA1 and is impaired by immune cells. *Stem Cells*. 2015;33:1277–1291. doi: 10.1002/stem.1916.
21. Davies BS, Beigneux AP, Barnes RH II, Tu Y, Gin P, Weinstein MM, Nobumori C, Nyrén R, Goldberg I, Olivecrona G, Bensadoun A, Young SG, Fong LG. GPIHBP1 is responsible for the entry of lipoprotein lipase into capillaries. *Cell Metab*. 2010;12:42–52. doi: 10.1016/j.cmet.2010.04.016.
22. Tontonoz P, Hu E, Devine J, Beale EG, Spiegelman BM. PPAR gamma 2 regulates adipose expression of the phosphoenolpyruvate carboxykinase gene. *Mol Cell Biol*. 1995;15:351–357.
23. Tontonoz P, Hu E, Spiegelman BM. Stimulation of adipogenesis in fibroblasts by PPAR gamma 2, a lipid-activated transcription factor. *Cell*. 1994;79:1147–1156.
24. Goto K, Iso T, Hanaoka H, et al. Peroxisome proliferator-activated receptor-γ in capillary endothelia promotes fatty acid uptake by heart during long-term fasting. *J Am Heart Assoc*. 2013;2:e004861. doi: 10.1161/JAHA.112.004861.
25. Martin G, Schoonjans K, Lefebvre AM, Staels B, Auwerx J. Coordinate regulation of the expression of the fatty acid transport protein and acyl-CoA synthetase genes by PPARalpha and PPARgamma activators. *J Biol Chem*. 1997;272:28210–28217.
26. Nielsen R, Pedersen TA, Hagenbeek D, Moulos P, Siersbaek R, Megens E, Denissov S, Børgesen M, Francoijs KJ, Mandrup S, Stunnenberg HG. Genome-wide profiling of PPARgamma:RXR and RNA polymerase II occupancy reveals temporal activation of distinct metabolic pathways and changes in RXR dimer composition during adipogenesis. *Genes Dev*. 2008;22:2953–2967. doi: 10.1101/gad.501108.
27. Enge M, Arda HE, Mignardi M, Beausang J, Bottino R, Kim SK, Quake SR. Single-cell analysis of human pancreas reveals transcriptional signatures of aging and somatic mutation patterns. *Cell*. 2017;171:321.e14–330.e14. doi: 10.1016/j.cell.2017.09.004.
28. Luconi M, Cantini G, Serio M. Peroxisome proliferator-activated receptor gamma (PPARgamma): is the genomic activity the only answer? *Steroids*. 2010;75:585–594. doi: 10.1016/j.steroids.2009.10.012.
29. Ricote M, Glass CK. PPARs and molecular mechanisms of transrepression. *Biochim Biophys Acta*. 2007;1771:926–935. doi: 10.1016/j.bbalip.2007.02.013.
30. Armoni M, Harel C, Karni S, Chen H, Bar-Yoseph F, Ver MR, Quon MJ, Karnieli E. FOXO1 represses peroxisome proliferator-activated receptor-gamma1 and -gamma2 gene promoters in primary adipocytes. A novel paradigm to increase insulin sensitivity. *J Biol Chem*. 2006;281:19881–19891. doi: 10.1074/jbc.M600320200.
31. Dowell P, Otto TC, Adi S, Lane MD. Convergence of peroxisome proliferator-activated receptor gamma and Foxo1 signaling pathways. *J Biol Chem*. 2003;278:45485–45491. doi: 10.1074/jbc.M309069200.
32. Fan W, Imamura T, Sonoda N, Sears DD, Patsouris D, Kim JJ, Olefsky JM. FOXO1 transrepresses peroxisome proliferator-activated receptor gamma transactivation, coordinating an insulin-induced feed-forward response in adipocytes. *J Biol Chem*. 2009;284:12188–12197. doi: 10.1074/jbc.M808915200.
33. Potente M, Mäkinen T. Vascular heterogeneity and specialization in development and disease. *Nat Rev Mol Cell Biol*. 2017;18:477–494. doi: 10.1038/nrm.2017.36.
34. Cao Y. Adipose tissue angiogenesis as a therapeutic target for obesity and metabolic diseases. *Nat Rev Drug Discov*. 2010;9:107–115. doi: 10.1038/nrd3055.
35. Sun K, Wernstedt Asterholm I, Kusminski CM, Bueno AC, Wang ZV, Pollard JW, Brekken RA, Scherer PE. Dichotomous effects of VEGF-A on adipose tissue dysfunction. *Proc Natl Acad Sci USA*. 2012;109:5874–5879. doi: 10.1073/pnas.1200447109.

36. Minchin JE, Dahlman I, Harvey CJ, Mejhert N, Singh MK, Epstein JA, Arner P, Torres-Vázquez J, Rawls JF. Plexin D1 determines body fat distribution by regulating the type V collagen microenvironment in visceral adipose tissue. *Proc Natl Acad Sci USA*. 2015;112:4363–4368. doi: 10.1073/pnas.1416412112.
37. Seki T, Hosaka K, Lim S, et al. Endothelial PDGF-CC regulates angiogenesis-dependent thermogenesis in beige fat. *Nat Commun*. 2016;7:12152. doi: 10.1038/ncomms12152.
38. Jiang X, Ye X, Guo W, Lu H, Gao Z. Inhibition of HDAC3 promotes ligand-independent PPARγ activation by protein acetylation. *J Mol Endocrinol*. 2014;53:191–200. doi: 10.1530/JME-14-0066.
39. Walkey CJ, Spiegelman BM. A functional peroxisome proliferator-activated receptor-gamma ligand-binding domain is not required for adipogenesis. *J Biol Chem*. 2008;283:24290–24294. doi: 10.1074/jbc.C800139200.
40. Werman A, Hollenberg A, Solanes G, Bjorbaek C, Vidal-Puig AJ, Flier JS. Ligand-independent activation domain in the N terminus of peroxisome proliferator-activated receptor gamma (PPARgamma). Differential activity of PPARgamma1 and -2 isoforms and influence of insulin. *J Biol Chem*. 1997;272:20230–20235.
41. Al-Rasheed NM, Chana RS, Baines RJ, Willars GB, Brunskill NJ. Ligand-independent activation of peroxisome proliferator-activated receptor-gamma by insulin and C-peptide in kidney proximal tubular cells: dependent on phosphatidylinositol 3-kinase activity. *J Biol Chem*. 2004;279:49747–49754. doi: 10.1074/jbc.M408268200.
42. Lazennec G, Canaple L, Saugy D, Wahli W. Activation of peroxisome proliferator-activated receptors (PPARs) by their ligands and protein kinase A activators. *Mol Endocrinol*. 2000;14:1962–1975. doi: 10.1210/mend.14.12.0575.
43. Chan SS, Twigg SM, Firth SM, Baxter RC. Insulin-like growth factor binding protein-3 leads to insulin resistance in adipocytes. *J Clin Endocrinol Metab*. 2005;90:6588–6595. doi: 10.1210/jc.2005-0595.
44. Silha JV, Gui Y, Murphy LJ. Impaired glucose homeostasis in insulin-like growth factor-binding protein-3-transgenic mice. *Am J Physiol Endocrinol Metab*. 2002;283:E937–E945. doi: 10.1152/ajpendo.00014.2002.
45. Baker DJ, Wijshake T, Tchkonia T, LeBrasseur NK, Childs BG, van de Sluis B, Kirkland JL, van Deursen JM. Clearance of p16Ink4a-positive senescent cells delays ageing-associated disorders. *Nature*. 2011;479:232–236. doi: 10.1038/nature10600.
46. Xu M, Palmer AK, Ding H, Weivoda MM, Pirtskhalava T, White TA, Sepe A, Johnson KO, Stout MB, Giorgadze N, Jensen MD, LeBrasseur NK, Tchkonia T, Kirkland JL. Targeting senescent cells enhances adipogenesis and metabolic function in old age. *Elife*. 2015;4:e12997. doi: 10.7554/eLife.12997.
47. Xu M, Tchkonia T, Ding H, Ogrodnik M, Lubbers ER, Pirtskhalava T, White TA, Johnson KO, Stout MB, Mezera V, Giorgadze N, Jensen MD, LeBrasseur NK, Kirkland JL. JAK inhibition alleviates the cellular senescence-associated secretory phenotype and frailty in old age. *Proc Natl Acad Sci USA*. 2015;112:E6301–E6310. doi: 10.1073/pnas.1515386112.
48. Zhu Y, Tchkonia T, Pirtskhalava T, et al. The Achilles' heel of senescent cells: from transcriptome to senolytic drugs. *Aging Cell*. 2015;14:644–658. doi: 10.1111/acel.12344.
49. Viswakarma N, Jia Y, Bai L, Vluggens A, Borensztajn J, Xu J, Reddy JK. Coactivators in PPAR-regulated gene expression. *PPAR Res*. 2010;2010:250126.
50. Tsuchiya K, Ogawa Y. Forkhead box class O family member proteins: the biology and pathophysiological roles in diabetes. *J Diabetes Investig*. 2017;8:726–734. doi: 10.1111/jdi.12651.
51. Nakae J, Cao Y, Oki M, Orba Y, Sawa H, Kiyonari H, Iskandar K, Suga K, Lombes M, Hayashi Y. Forkhead transcription factor FoxO1 in adipose tissue regulates energy storage and expenditure. *Diabetes*. 2008;57:563–576. doi: 10.2337/db07-0698.
52. Nakae J, Kitamura T, Kitamura Y, Biggs WH III, Arden KC, Accili D. The forkhead transcription factor Foxo1 regulates adipocyte differentiation. *Dev Cell*. 2003;4:119–129.
53. Gealekman O, Guseva N, Gurav K, Gusev A, Hartigan C, Thompson M, Malkani S, Corvera S. Effect of rosiglitazone on capillary density and angiogenesis in adipose tissue of normoglycaemic humans in a randomised controlled trial. *Diabetologia*. 2012;55:2794–2799. doi: 10.1007/s00125-012-2658-2.

Highlights

- Native microvascular endothelial cells from human adipose tissue express actors of the fatty acids handling machinery at levels comparable to mature adipocytes.
- PPARG (peroxisome proliferator–activated receptor gamma) regulates fatty acid uptake in microvascular endothelial cells from human adipose tissue.
- Senescence blunts the regulation of fatty acid handling by PPARG in microvascular endothelial cells from human adipose tissue.
- Senescence favors the emergence of an inflammatory phenotype in response to PPARG agonist in microvascular endothelial cells from human adipose tissue.
- In the senescent human adipose tissue endothelial cell the alteration of PPARG nuclear translocation coincides with the accumulation of FOXO1 (forkhead box protein O1).

Arteriosclerosis, Thrombosis, and Vascular Biology

JOURNAL OF THE AMERICAN HEART ASSOCIATION

Senescence Alters PPARG (Peroxisome Proliferator–Activated Receptor Gamma)-Dependent Fatty Acid Handling in Human Adipose Tissue Microvascular Endothelial Cells and Favors Inflammation

Anaïs Briot, Pauline Decaunes, Fanny Volat, Chloé Belles, Muriel Coupaye, Séverine Ledoux and Anne Bouloumié

Arterioscler Thromb Vasc Biol. published online March 15, 2018;
Arteriosclerosis, Thrombosis, and Vascular Biology is published by the American Heart Association, 7272 Greenville Avenue, Dallas, TX 75231

Print ISSN: 1079-5642. Online ISSN: 1524-4636

SUPPLEMENTAL TABLES

Supplemental Table I- Clinical parameters from the donors used in Figure 2.

	Non-Obese	Obese
number	16	51
BMI	23.93 ± 0.67	43.54 ± 0.78
Age	42.44 ± 2.19	40.82 ± 1.37
Fasting glucose (mmol/L)	5.036 ± 0.10	5.363 ± 0.074
HbA1c (%)	5.372 ±0.082	5.662 ± 0.057
CRP (hs)	2.463 ± 0.514	8.608 ± 0.711
Triglycerides (mmol/L)	1.007 ± 0.147	1.283 ± 0.110
HDL (mmol/L)	1.606 ± 0.114	1.243 ± 0.046
LDL (mmol/L)	3.073 ± 0.161	3.324 ± 0.116
Cholesterol (mmol/L)	5.126 ± 0.223	5.142 ± 0.130
HOMA-IR	ND	4.559±0.46

Mean values ± standard errors are presented.

BMI: Body Mass Index. HbA1c: glycated hemoglobin. CRP (hs): C-Reactive Protein high-sensitivity. HDL: High Density Lipoprotein. LDL: Low Density Lipoprotein. HOMA-IR: homeostasis model assessment of insulin resistance.

Supplemental Table II- Probe and primer sets used for quantitative RT-PCR

Target gene	Probe/Primer set
18S	Cat # 4352930E
CD31	Hs00169777-m1
CD36/FAT	Hs00169627-m1
CCND1	Hs00277039-m1
CDKN2A	Hs00923894-m1
FABP4/AP2	Hs01086177-m1
FOXO1	Hs01054576-m1
GPIHBP1	Hs01564843-m1
ICAM1	Hs00164932-m1
IGFBP3	HS00181211-m1
IL6	Hs00174131-m1
IL8	Hs00174103-m1
MCP1	Hs00234140_m1
NFKBIA	Hs00153283_m1
PPARG	Hs00234592-m1
PPIB	Hs00168719-m1
SIRT1	Hs00202021-m1
SCL27A1	Hs01587917-m1
SLC27A3	Hs00950760-g1
SLC27A4	Hs00192700-m1